Experimental examination of dipole-dipole cross-correlations by dielectric spectroscopy, depolarized dynamic light scattering, and computer simulations of molecular dynamics

K. Koperwas [1,*] J. Gapiński [2] Z. Wojnarowska,[1] A. Patkowski [2] and M. Paluch [1]

[1]*Institute of Physics, University of Silesia in Katowice, 75 Pułku Piechoty 1, 41–500 Chorzow, Poland*
[2]*Faculty of Physics, Adam Mickiewicz University, Uniwersytetu Poznańskiego 2, 61–614 Poznań, Poland*

The contribution of *cross-* and *self*-correlations to the dielectric and light-scattering spectra of supercooled polar glass formers has recently become a most challenging problem. Herein, we employ dielectric spectroscopy, depolarized dynamic light scattering (DDLS), and rheology to thoroughly examine the dynamics of van der Waals liquid 1,2-Diphenylvinylene. Carbonate (DVC), which is a polar counterpart of canonical glass former ortho-Terphenyl (OTP). We show that the light-scattering data correspond well with the dielectric permittivity function over a wide T range. This pattern is very different from the peaks' separation $\omega_{\max}^{\mathrm{DDLS}}/\omega_{\max}^{\mathrm{BDS}} = 3.7$ reported recently for tributyl phosphate (TBP), despite the same dielectric characteristics of these two glass formers ($\beta_{\mathrm{KWW}} = 0.75$, $\Delta\varepsilon = 20$ for both TBP and DVC; KWW stands for Kohlrausch-Williams-Watts). This indicates different influence of orientational correlations in both methods for these two systems. We also show the results of the computer simulations of the model, polar molecules, which clearly indicate that the contribution of the cross-term to the correlation function probed in the DDLS experiment can be significant.

I. INTRODUCTION

Molecular dynamics of glass-forming liquids has been routinely investigated through a broadband dielectric spectroscopy (BDS). The main reasons for employing this technique is an impressive available frequency range (from 10^{-6} to 10^{12} Hz [1]) and the fact that it delivers information on the orientational correlations between molecules. They are included in the dielectric relaxation strength [2] and parametrized by the Kirkwood correlation factor, whereas the character of the molecular dynamics is deduced from the dielectric loss spectrum. In the case of nonionic systems, the molecular mobility probed by BDS is related to the molecular reorientation, which is manifested in the dielectric loss spectrum as a relaxation peak [3].

Analogically to the BDS experiment, which probes the changes of system's total dipole moment, using depolarized dynamic light scattering (DDLS) one can estimate the depolarized component of the scattered-light signal for the studied system. Typically, a symmetric top molecule's reorientation dynamics is probed in the right-angle I_{VH} geometry; that is, when scattered light is detected at the right angle, the incident light is polarized perpendicular to the scattering plane ("V") and the scattered light is analyzed only for polarization parallel to the scattering plane ("H"). As a symmetric top, a molecule possesses two different components of the optical polarizability tensor: $\alpha_\parallel$ parallel to its symmetry axis (collinear with the unit vector $\boldsymbol{u}$ defining the direction of the dipole moment $\boldsymbol{\mu}$) and $\alpha_\perp$ in any direction perpendicular to this axis. Scattered signal fluctuations arise from the fact that the dipole-moment component perpendicular to incident light

polarization plane (being the source of depolarized signal) depends on the orientation of the polarizability tensor (and hence the molecule). Such phenomenon does not occur for optically isotropic molecules, so the anisotropy is absolutely necessary to perform a DDLS experiment, however not required in simulation studies. Typical description of DDLS correlation function is limited only to slow processes like rotational diffusion. Other processes that also contribute to the DDLS spectrum, like dipole-induced-dipole, Raman, and Brillouin scattering, are not included in this description due to much higher frequency and much lower amplitude [4,5]. It has been shown that in the discussed geometry the effective component of the dipole moment induced in the ith molecule is proportional to the factor $\alpha_{yz}(t) = \beta u_y(t)u_z(t)$, where $\beta = \alpha_\parallel - \alpha_\perp$ is the optical anisotropy [6]. There are usually two types of relaxation processes: primary α relaxation and secondary β mode [7–9]. The first one plays a pivotal role in describing the vitrification process of liquid because it mimics the liquid structure reorganization. Therefore, it is also called structural relaxation. A characteristic feature of the α-relaxation process obtained from dielectric measurements in the vicinity of glass-transition temperature, T_g, is a non-Debye shape [10] usually quantified by the exponent β_{KWW} in empirical Kohlrausch-Williams-Watts (KWW) function $C(t) = Ae^{-(t/\tau_{\mathrm{KWW}})^{\beta_{\mathrm{KWW}}}}$ modeling the time autocorrelation function related to the BDS permittivity spectrum by Fourier transform. Although the deviation from the Debye behavior is a material-dependent feature, it was experimentally established that for van der Waals liquids it was often related to the molecular polarity. In Ref. [11] the authors observed that the increase of the dipole moment is accompanied by a narrowing of an α-relaxation peak, i.e., $\beta_{\mathrm{KWW}}^{\mathrm{BDS}}$ increased from 0.4 to 0.9 within the set of studied liquids. This is a quite striking observation, bearing in mind the results obtained from the measurements

*Corresponding author: kajetan.koperwas@us.edu.pl

by means of depolarized dynamic light scattering, which also probes the (re)orientational collective dynamics [12]. In contrast to BDS findings, only very weak variation in $\beta_{\text{KWW}}^{\text{DDLS}}$ was found, explicitly $\beta_{\text{KWW}}^{\text{DDLS}} = 0.58 \pm 0.06$ in all studied compounds.

Recently, many attempts have been made to explain the discrepancies between BDS and DDLS spectra [13–15]. The time autocorrelation functions $C^{\text{BDS}}(t)$ and $C^{\text{DDLS}}(t)$ can be expressed as a sum of the self- and cross-correlation functions. For the sake of notation simplicity, we use $C'^{\text{BDS}}(t)$ and $C'^{\text{DDLS}}(t)$ functions, which are normalized such that the respective "self-" part has an amplitude equal to 1:

$$C'^{\text{BDS}}(t) = C_{\text{self}}^{\text{BDS}}(t) + C_{\text{cross}}^{\text{BDS}}(t)$$
$$= \frac{1}{N\mu^2}\left\langle \sum_i \boldsymbol{\mu}_i(0)\cdot\boldsymbol{\mu}_i(t) \right\rangle$$
$$+ \frac{1}{N\mu^2}\left\langle \sum_i \sum_{j\neq i} \boldsymbol{\mu}_i(0)\cdot\boldsymbol{\mu}_j(t) \right\rangle, \quad (1)$$

$$C'_{\text{DDLS}}(t) = C_{\text{self}}^{\text{DDLS}}(t) + C_{\text{cross}}^{\text{DDLS}}(t)$$
$$= \frac{1}{N}\left\langle \sum_i u_{z,i}(0)u_{y,i}(0)u_{z,i}(t)u_{y,i}(t) \right\rangle$$
$$+ \frac{1}{N}\left\langle \sum_i \sum_{j\neq i} u_{z,i}(0)u_{y,i}(0)u_{z,j}(t)u_{y,j}(t) \right\rangle. \quad (2)$$

It was postulated that the two contributions can be resolved as separate processes in the measured BDS permittivity spectrum [16,17]. However, no explanation was given why this effect occurs only in the BDS signal, despite the fact that both BDS and DDLS measure collective reorientation dynamics. It was further suggested that the cross-correlations process has a Debye-like shape, and its intensity dominates the dielectric permittivity spectrum when the molecular polarity is high [16,17]. No arguments explaining the abandonment of the standard, well-established models of single-process collective dynamics [4,18] were given [17].

In this context, it is worth mentioning that the existence of two processes in BDS permittivity spectrum has also been predicted by the theory developed by Déjardin *et al.* [19,20], according to which the response of a pair of dipoles consists of the two relaxation processes associated with the single- and collective molecular motions. The relaxation times of those processes depend on the parameter $\lambda \sim \mu^2$ (μ is a molecular dipole moment), increase of which separates their timescales. One should note, however, that in the current state of this theory the separation between those processes typically reaches many orders of magnitude (up to several tens of orders for realistic values of λ for systems with large dipole moments), which should make the slower mode that is hidden in the conduction band undetectable.

From the experimental point of view, any technique can measure only one main reorientation process (self- or collective), moreover "filtered" by the appropriate associated Legendre polynomial. Using the formalism of spherical harmonics, Eqs. (1) and (2) can be expressed in terms of appropriate Legendre polynomial:

$$C'_{\text{BDS}}(t) = \frac{1}{N}\left(\left\langle \sum_i P_1(\boldsymbol{u}_i(0)\cdot\boldsymbol{u}_i(t)) \right\rangle \right.$$
$$\left. + \left\langle \sum_i \sum_{j\neq i} P_1(\boldsymbol{u}_i(0)\cdot\boldsymbol{u}_j(t)) \right\rangle\right), \quad (3)$$

$$C'_{\text{DDLS}}(t) = \frac{1}{N}\left(\left\langle \sum_i P_2(\boldsymbol{u}_i(0)\cdot\boldsymbol{u}_i(t)) \right\rangle \right.$$
$$\left. + \left\langle \sum_i \sum_{j\neq i} P_2(\boldsymbol{u}_i(0)\cdot\boldsymbol{u}_j(t)) \right\rangle\right). \quad (4)$$

As one can see, BDS measures collective reorientations filtered by the P_1 polynomial [$P_1(x) = x$], whereas DDLS measures the same collective reorientations filtered by the P_2 polynomial [$P_2(x) = (3x^2 - 1)/2$], which usually results in different mean relaxation times obtained from these two methods but also in different relative contributions of cross-correlations to the respective total signal. The argument x of both polynomials is equal to $\cos\theta$, where θ is an angle between dipole moments of system's molecules. The well-established standard BDS and DDLS theories predict a single process for collective molecular reorientation. Also, a single process is predicted for the self-reorientation dynamics, the measurement of which requires either a dedicated technique (e.g., NMR) or fulfilling special conditions in which the *collective* dynamics reduces to single-molecule (self-) dynamics for a given technique. This reduction may result from the weakness of intermolecular interactions or from the filtering effect of the appropriate Legendre polynomial. Very often DDLS results are erroneously classified as self- (single molecule). It is possible and probably quite common that the P_2 collective correlation function possesses negligible P_2 cross-term, but formally that is not always true and cannot be assumed *a priori* for every sample. The cross-term is just a complementary factor, which can possibly exhibit a negative amplitude and a complex temporal behavior. Supercooling of liquids may lead to its enhancement due to densification of the system and resulting increase of intermolecular interactions. In regular liquids, by no means can the collective correlation function be a sum of two exponential processes, i.e., of the exponential self- term and some additional component resulting from the cross-correlations [4,18,21] It is not clear yet whether the broadening of relaxation times in supercooled liquids changes the situation in this respect; however, no solid justification of such "process bifurcation" in the collective correlation function has been given so far.

To complete these introductory considerations, we should mention here the static orientational correlation factors and relations between different measures of relaxation time. Concerning the correlation factors, we have the Kirkwood-Fröhlich correlation factor g_K (denoted g_1 from now on) in BDS and its DDLS counterpart (without a dedicated name), denoted here as g_2. Their physical interpretation can be expressed such that

$$g_l - 1 = A_c^{(l)}/A_s^{(l)}, \quad (5)$$
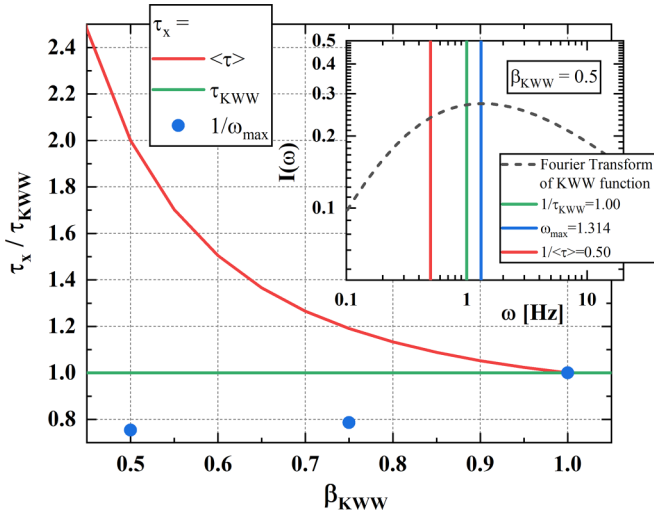
FIG. 1. Mutual dependencies of $\langle\tau\rangle$, τ_{KWW}, and $1/\omega_{\max}$ for processes described by KWW correlation functions characterized by different β_{KWW} values. Inset: Shape of the dielectric loss spectrum for a process characterized by KWW correlation functions with $\beta_{\mathrm{KWW}} = 0.5$ with lines indicating $\omega_{\max}$ and reciprocal values of $\langle\tau\rangle$ and τ_{KWW}.

where $A_c^{(l)}$ and $A_s^{(l)}$ are the amplitudes of the cross- and self-contributions to static orientational correlations, respectively. Index "l" ($l = 1, 2$) denotes the degree of Legendre polynomial, and hence the method ($l = 1$ for BDS and $l = 2$ for DDLS). Those amplitudes are equal to the contributions of the respective terms in the collective correlation functions $C'^{\mathrm{BDS}}(t)$ and $C'^{\mathrm{DDLS}}(t)$ [Eqs. (3) and (4)]. Concerning the measures of relaxation time, the most frequently used are τ_{KWW}, $1/\omega_{\max}$, and the mean relaxation time $\langle\tau\rangle$ defined as the integral of the normalized correlation function, which for the KWW model turns into $\langle\tau\rangle = \frac{\tau_{\mathrm{KWW}}}{\beta_{\mathrm{KWW}}}\Gamma(\frac{1}{\beta_{\mathrm{KWW}}})$. The relations of these three parameters, calculated analytically or numerically (fast Fourier transform), are shown in Fig. 1 for three values of the β_{KWW} parameter.

As one can see in the main panel of Fig. 1, the values of τ_{KWW} and $1/\omega_{\max}$ are quite close even for low β_{KWW} values. However, any thorough comparison of relaxation times should be made on the level of $\langle\tau\rangle$ values, so for systems with relatively low β_{KWW} values, where the difference between $\langle\tau\rangle$ and $1/\omega_{\max}$ can be as large as a factor of 2.7 for $\beta_{\mathrm{KWW}} = 0.5$, this correction should be included. For example, the popular method of superimposing loss-spectra peaks to prove the equality of relaxation times is correct only for systems with similar β_{KWW} values. On top of these relations, one should also include the method-related differences in mean relaxation times. The different order of Legendre polynomial present in the models describing BDS and DDLS dynamics of reorientation introduces additional parameter $\kappa = \langle\tau_s^{(1)}\rangle/\langle\tau_s^{(2)}\rangle$, which can range from $\kappa = 3$ in the limit of small-step diffusion to $\kappa = 1.57$ in the big-step diffusion limit [22], or even 1 for some model cases [23]. As in very viscous liquids the big-step diffusion model is expected [22], the commonly accepted approximation is that the κ parameter is slightly larger than 1. In further analysis a value $\kappa = 1.57$ (denoted as "standard") will be used for estimation of other parameters; however, we

are aware that for every molecule this parameter may have a different (and temperature-dependent) value, most probably in the range $1.57 < \kappa < 3$.

Collective relaxation times in dipolar liquids may be strongly affected by static and—-to a much lesser extent—-dynamic correlation factors. Ignoring the dynamic ones [4], the ratio of BDS to DDLS collective relaxation times can be expressed as

$$\frac{\langle\tau^{\mathrm{BDS}}\rangle}{\langle\tau^{\mathrm{DDLS}}\rangle} = \frac{\langle\tau_s^{\mathrm{BDS}}\rangle}{\langle\tau_s^{\mathrm{DDLS}}\rangle}\frac{g_1}{g_2} = \kappa\,\frac{g_1}{g_2}. \qquad (6)$$

Note that for systems where $\beta_{\mathrm{KWW}}^{\mathrm{BDS}} > \beta_{\mathrm{KWW}}^{\mathrm{DDLS}}$, and correlations are weak ($g_1 = g_2 \cong 1$), parameter κ and the ratio $\langle\tau\rangle/(1/\omega_{\max})$ may roughly compensate each other, which results in equal values of $1/\omega_{\max}$ from BDS and $\langle\tau\rangle$ from DDLS measurements. This observation may explain why activation plots composed of these two parameters often overlap very well.

In this paper we show the results of BDS and DDLS experiments performed for the structurally analogical systems which differ in molecular polarity. Interestingly, the positions of the main peaks of BDS and DDLS spectra correspond to each other for both studied materials. Even more, this correspondence is held for many decades of relaxation times and is fulfilled also for the relaxation time determined from the rheology experiment. Apparently, the only difference between obtained BDS and DDLS spectra is in their shapes. This picture changes when mean relaxation times are compared. For ortho-Terphenyl (OTP) the small dipole-moment value practically excludes interaction-induced orientational correlations, so both methods presumably measure mainly the self-dynamics. Hence, the ratio of mean relaxation times corresponds to a value κ resulting solely from the difference in quantities measured by BDS and by DDLS. More interesting is the result obtained for 1,2-Diphenylvinylene Carbonate (DVC) (strong dipole), which seems to show that irrespective of the suggestions that DDLS measures only the self-dynamics, it is DDLS in this case that senses strong orientational cross-correlations, resulting in retarded collective dynamics, while BDS measures only the self-dynamics. To support this conclusion, we show the outcomes of the computer simulations of the molecular dynamics performed for the polar highly symmetric molecule, for which we calculate the self- and cross-contributions to the Legendre polynomials of the first and second order. Obtained results prove that P_2 polynomial may provide a substantial cross-term, strongly contributing to the collective DDLS signal.

II. EXPERIMENT

A. Materials

The first material we chose for our studies was the well-known canonical glass former OTP. All experimental data for OTP were taken from literature: dipole moment, $\mu = 0.2D$ from Ref. [24] and BDS and DDLS results from Refs. [20–23]). The choice of the second system, which was DVC, was dictated by the conception of examining a molecule structurally similar to OTP but possessing a bigger dipole moment. DVC was purchased from Sigma-Aldrich and
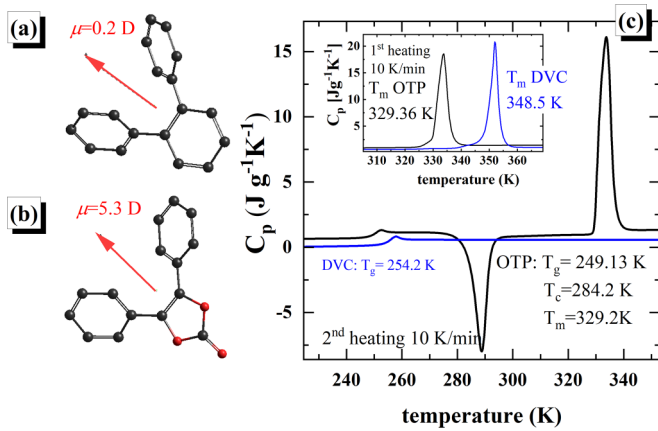
FIG. 2. Panels (a) and (b) depict the molecular structures of OTP and DVC, respectively. The red arrows indicate the direction of the dipole moment. Panel (c) presents the thermograms of both studied glass formers. In the inset, the initial heating of the crystallized sample T_g is presented for OTP and DVC.

used as received. As shown in Figs. 2(a) and 2(b), the only difference between these two molecules lies in the type of middle ring, i.e., the polar dioxolane for DVC vs the nonpolar phenyl for OTP [25]. This seemingly minor change brings a substantial increase in dipole moment for DVC ($\mu = 5.3D$). At the same time, two nonpolar aromatic rings make both molecules highly optically anisotropic. Since the lateral rings are rotated out of the central ring plane, the overall shape of OTP and DVC comes close to a sphere [26]. In this way, it is believed that the dynamical properties of OTP can be ascribed as generic properties of the glass-forming liquids, which do not depend on microscopic structural peculiarities [26].

B. Methods

1. Differential scanning calorimetry measurements

The thermodynamic properties of DVC were examined by means of a Mettler-Toledo differential scanning calorimetry (DSC) instrument equipped with a liquid-nitrogen cooling accessory. The calibrations for temperature and enthalpy were performed by using indium and zinc standards. The crystalline sample was placed in an aluminum pan and heated at the rate of 10 K/min up to 380 K. After that, cooling and subsequent heating scans were performed.

2. Dielectric measurements

The dielectric measurements were performed using a Novo-Control GMBH Alpha dielectric spectrometer in a wide frequency range from 10^{-2} to 10^7 Hz. The stainless-steel electrodes (diameter = 15 mm) had a fixed distance of 0.1 mm maintained by the use of calibrated width silica fibers. During the measurements, the temperature was controlled by a Novocool system using a nitrogen gas cryostat with an accuracy of 0.1 K.

3. Dynamic depolarized light scattering

The DDLS measurements were performed in a homemade cryochamber cooled by a Peltier plate. The temperature read-

out accuracy was 0.1 K. The temperature was calibrated in the following way: during the test procedure an additional calibrated thermocouple sensor was immersed in a glycerol sample placed directly in the measuring cuvette in the scattering volume. The indications of the thermocouple were compared with the standard PT100 sensor (placed close to but outside the cell) used to stabilize the temperature in the cell. A calibration curve was created for the entire available temperature range. In the standard measurements the temperature from the calibration curve was used as a correct temperature value for a given PT100 indication. Light of 660-nm wavelength from an Obis laser (Coherent, USA) was focused on the sample maintained in a quartz rectangular cuvette (Hellma, Germany). Light scattered in the *VH* geometry was collected by a collimator connected to an optical fiber splitter (Schäfter+Kirchhoff GmbH, Germany) and directed to two avalanche photodiodes (SPCM-AQR, Perkin Elmer), providing the possibility for pseudo–cross-correlation mode of operation of the ALV7000 digital correlator (ALV, Germany). This mode of operation reduces the afterpulsing effects occurring in the detectors, providing a safe way to measure the correlation functions starting from the first channel of the correlator (12.5 ns). The measured second-order (intensity) correlation functions $g^{(2)}(t)$ were analyzed using the Siegert relation and the KWW model for $g^{(1)}(t)$ in the native software of the correlator. From this fit the parameters τ_{KWW} and β_{KWW} were obtained. The corresponding DDLS spectra $I(\omega)$ were calculated as Fourier transforms of the $g^{(1)}(t)$ and the susceptibility $\chi''(\omega) = \omega I(\omega)$ was obtained.

4. Viscosity measurements

The viscosity was measured employing an ARES G2 Rheometer. In the supercooled-liquid region, aluminum parallel plates of diameter 4 mm were used. The rheological experiments were performed in the frequency range from 0.1 to $100 \, \text{rad s}^{-1}$ (10 points per decade) with strain equal to 0.01% in the vicinity of the liquid-glass transition.

5. Molecular dynamics simulations

The studied system consists of 14400 quasireal tetrahedron-like molecules (TMs), which are created from five identical atoms characterized by the mass of the carbon atom in the benzene ring. This choice means that consistency between the repulsive and dispersion interactions, as well as the length, rigidity, and flexibility of bonds, is naturally assured if one parametrizes those interactions using OPLS-AA force-field parameters delivered for the carbon atom of the benzene ring [27]. The only modification of the mentioned parameters refers to atoms' charges, which are set to $0.0e$ for three side atoms, whereas the charge of the central atom equals $0.75e$ for the second TM system. Consequently, the remaining side atom possesses charge equal to $-0.75e$. In this way the studied TM seems to be an analog of the DVC particle because it is spherically symmetric and possesses permanent dipole moment $\mu = 5D$. The molecular dynamics simulations are performed using the GROMACS software [28–32] in the NVT ensemble with the Nosé-Hoover thermostat [33–35]. The equations of motion were integrated using the velocity-Verlet algorithm [36] with a time step equal

to 0.001 ps and truncation of the intermolecular interaction at a distance equal to 4.26 nm, which is 12 times higher than the σ parameter of the intermolecular interaction potential. The long-range Coulomb interactions are taken into account employing the particle mesh Ewald summation method considering tinfoil conditions [37]. The systems' volume is equal to 1442.897 nm^3, whereas the temperature $T = 360$ K.

III. RESULTS

In the first step of our studies, we identify the glass-forming ability of DVC. For this purpose, the standard DSC scans have been performed. As seen in the inset to Fig. 2(c), heating of crystalline powder with the standard rate of 10 K/min brings an endothermic peak with the onset at 348.5 K, which is 19 K higher than the melting point of OTP ($T_m = 329.4$ K). The second heating scan, performed after quenching of melted materials, is presented in Fig. 1(c). The midpoint of a step-like increase in heat capacity provides the temperature of liquid-glass transition. It is equal to 254.2 K for DVC, and interestingly, it is only 5 K above that of OTP. However, in contrast to OTP, DVC does not reveal cold crystallization during the heating process. Hence, we can conclude that DVC is relatively easy to supercool. Moreover, the temperature range at which it persists in a supercooled state is similar to that of OTP, and therefore it becomes an excellent material for further spectroscopic studies.

In the next step, we carried out the dielectric, DDLS, and mechanical measurements to examine the molecular dynamics of supercooled DVC. The representative results are plotted in Fig. 3(a). As shown, the imaginary part of complex dielectric permittivity $\varepsilon''(f)$ takes the form of a well-resolved peak, so-called structural α relaxation, which shifts toward higher frequencies on heating. Similar results have been obtained from rheology [Fig. 3(b)]; however, here, the mechanical shear modulus peaks $G''(f)$ can be monitored only within four decades of frequency from T_g. In contrast to dielectric and mechanical data, the results of the DDLS experiment are presented in the time domain. The obtained intensity-intensity autocorrelation function $g^{(2)}(t) - 1$, illustrated in Fig. 3(c), has been parametrized by the KWW function fit to the corresponding $g^{(1)}(t)$.

IV. DISCUSSION

The first observation discussed here is the effect of molecules' polarity on the dielectric response function. To address this issue, we compared the spectra of DVC and OTP recorded at the same frequency of ε'' maximum, that is, at the same distance from liquid-glass transition (see Fig. 4). Note that the BDS data for OTP were taken from the literature [38].

As can be seen, the replacement of the phenyl ring by highly polar vinylene carbonate brings a substantial increase in dielectric strength and narrowing of the $\varepsilon''(f)$ function. Namely, the $\beta_{KWW}^{BDS} = 0.75$ and $\Delta\varepsilon = 20$ for DVC, while $\beta_{KWW}^{BDS} = 0.5$ has been reported for OTP in Ref. [39]. Consequently, a correlation between μ and β_{KWW}^{BDS} suggested in Ref. [11] is satisfied.

Now, we directly compare the BDS and DDLS susceptibility spectra of a given material recorded at the same
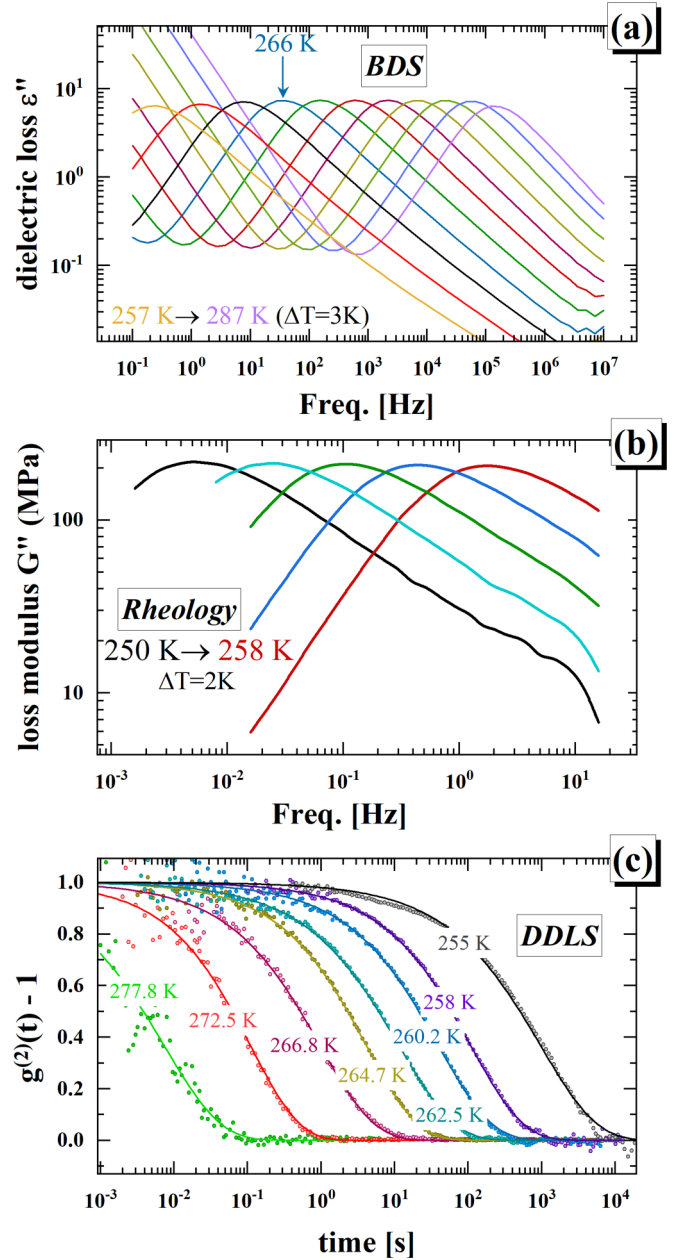
FIG. 3. Panel (a) presents the dielectric permittivity spectra of DVC measured at the temperature range from 257 to 287 K. The blue arrow indicates the permittivity spectrum used in our further analysis. Panel (b) shows the representative mechanical shear modulus spectra of DVC. Panel (c) shows normalized intensity-intensity autocorrelation function (points) measured at temperatures corresponding to the BDS measurements for DVC. The lines present the fits of the KWW function to experimental data with the use of Siegert relation, as described in Sec. II B, Methods.

temperature. For OTP, we used the literature data reported in Refs. [38–41]. At first glance, there is an accordance between the position of BDS and DDLS modes, i.e., $f_{max}^{BDS} \approx f_{max}^{DDLS}$. However, at the same time the BDS permittivity spectrum of OTP is broader than the DDLS one, $\beta_{KWW}^{BDS} = 0.50$ vs $\beta_{KWW}^{DDLS} = 0.59$. Using the relation $\langle\tau\rangle\omega_{max}(\beta_{KWW})$ presented in Fig. 1, we calculate for OTP the ratio of mean relaxation times $\frac{\langle\tau^{BDS}\rangle}{\langle\tau^{DDLS}\rangle} = 1.4$. Taking the standard value of $\kappa = 1.57$,
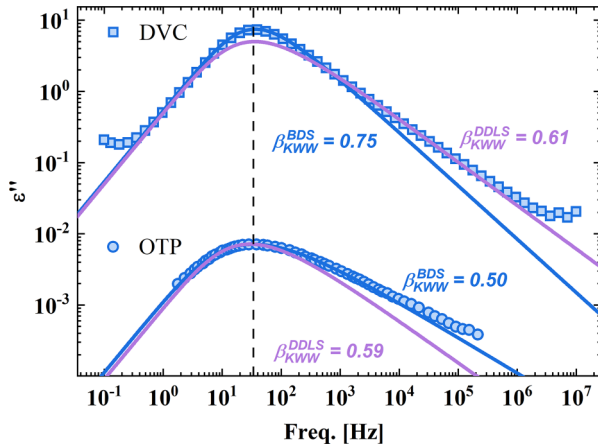
FIG. 4. The loss part of the dielectric spectra measured at the temperature equal to 258 and 266 K for OTP and DVC, respectively. The blue lines are the fits of the KWW function to BDS data. The violet lines represent the DDLS susceptibility results. Data for OTP were taken from Refs. [20–23].

we use Eq. (6) to calculate the value of $g_1/g_2 = 0.9$. As the value $g_1 = 1$ is a reasonable assumption for OTP, within experimental error and adopted approximation, we conclude that both methods measure only the self- component of respective correlation function and no cross-terms can be detected.

To examine the DVC case, first we fit the KWW function to the $g^{(1)}(t)$ function [corresponding to the measured $g^{(2)}(t) - 1$] and use the Fourier transform to convert the fit to the spectrum $I(\omega)$ and susceptibility $\omega I(\omega)$ in the frequency domain. This procedure has been applied to DDLS data recorded at 266 K. Subsequently, the obtained susceptibility spectrum is shifted vertically to cover the high-frequency flank of $\varepsilon''(f)$ function registered at the same T conditions (see Fig. 3). Note that special attention has been paid to temperature calibration in BDS and DDLS setups. As it can be observed, the DDLS susceptibility spectrum of DVC is broader than the dielectric permittivity function ($\beta_{KWW}^{BDS} = 0.75$ vs $\beta_{KWW}^{DDLS} = 0.61$). The positions of BDS and DDLS α peaks are almost identical. Interestingly, similar relations were also reported for Cresolphthaleine-dimethyl-ether (KDE) and Phenolphthaleine-dimethyl-ether (PDE) [42]. The hint for understanding these results might be that DVC, PDE, and KDE's chemical structures contain aromatic moieties, which are not present in the chemical structure of tributyl phosphate, for which peak separation $\omega_{max}^{DDLS}/\omega_{max}^{BDS} = 3.7$ was reported. For DVC the ratio of mean relaxation times calculated using the relation $\langle\tau\rangle\omega_{max}(\beta_{KWW})$ (see Fig. 1) amounts to $\frac{\langle\tau^{BDS}\rangle}{\langle\tau^{DDLS}\rangle} = 0.8$. Taking the standard value of $\kappa = 1.57$, we calculate [Eq. (6)] the ratio $g_1/g_2 = 0.5$. Full quantitative comparison of the BDS and DDLS spectra based on Fig. 1 and Eq. (6) can be performed if all necessary parameters are available.

Summarizing, the two crucial observations can be made from Fig. 3. The first is that the DDLS susceptibility spectrum for OTP, a weakly polar liquid, is narrower than the BDS permittivity spectrum. The second is that although the positions of the main peaks of BDS and DDLS spectra are almost identical for both materials independent of the μ value, the ratio of mean relaxation times allows to estimate
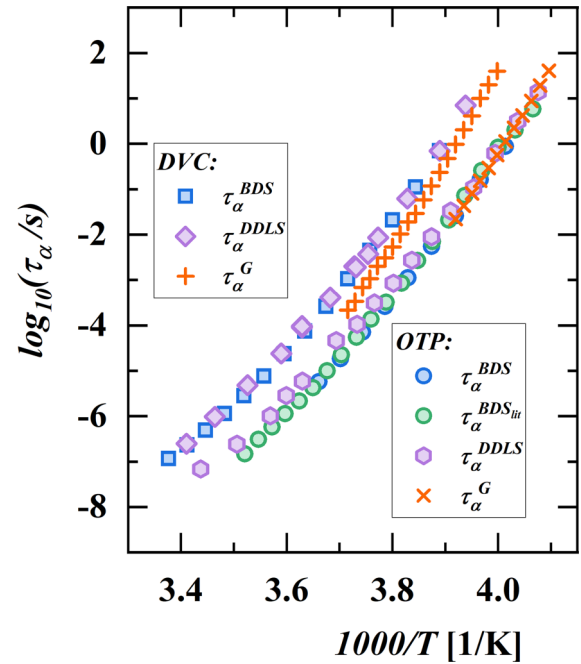
FIG. 5. The structural relaxation times for OTP and DVC determined by dielectric spectroscopy ($1/\omega_{max}$), DDLS $\langle\tau\rangle$, and rheology. The literature results for OTP are taken from Ref. [38].

$g_1/g_2 \cong 1$ for OTP and $g_1/g_2 \cong 0.5$ for DVC. Analyzing this result, one should remember that despite very large value of the dipole moment in DVC, the g_1 value obtained from ε' measurements reaches only $g_1 = 1.04$, indicating an apparent lack of orientational correlations detected by BDS. Note that the similar g_1 values, i.e., values close to 1, have been reported for propylene-carbonate, a significantly strongly polar liquid [43–45]. On the other hand, the value of $g_2 = 2g_1 \cong 2$ clearly shows strong correlations detected by DDLS. This apparent discrepancy can be qualitatively illustrated using the hypothetical example of antiparallel orientation of dipoles, resulting in negative correlations detected by BDS and positive correlations detected by DDLS, because light scattering is not sensitive to such differentiation (alignment is enough). In the case of DVC such partially antiparallel and partially parallel orientation of dipoles could explain observed results. More formally, it is the shape of the Legendre polynomial that provides the weight to angular correlations, P_1 for BDS and P_2 for DDLS.

In Fig. 5 we present the temperature dependence of the BDS and DDLS relaxation times. The first conclusion gained from this figure is that at the given T, the relaxation times for DVC are longer than for OTP, which is due to dipole-dipole interactions slowing down molecular dynamics [46,47]. This observation is true regardless of the measure of relaxation time, as the separation is substantial. The agreement between measured timescales, i.e., $\tau_\alpha^{BDS} = 1/\omega_{max}$ and $\tau_\alpha^{DDLS} = \langle\tau^{DDLS}\rangle$, is satisfied in a wide range of temperatures for DVC and OTP.

A hint concerning the actual relations between $\langle\tau^{BDS}\rangle$ and $\langle\tau^{DDLS}\rangle$ and the values of static correlation factors can be obtained using the computer simulations of molecular dynamics, which ensure access to all molecular coordinates and
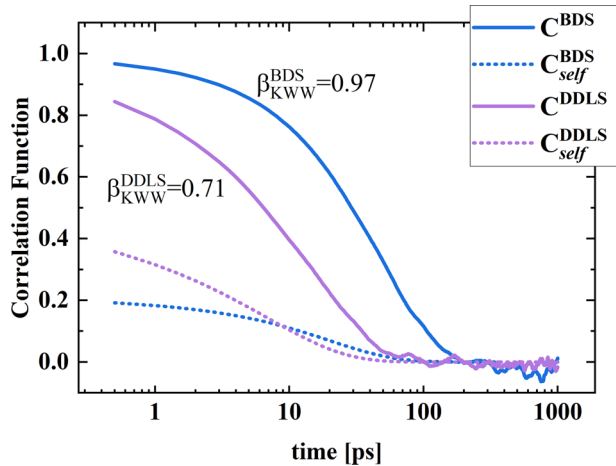
FIG. 6. The correlation functions probed in the BDS and DDLS experiment and their self- components for studied TM systems. Note that both DDLS functions are the $g^{(1)}(t)$ correlation functions. Both collective correlation functions were normalized to 1.

their time evolution. Consequently, this method enables calculation of all kinds of time correlation functions. Therefore, not only the collective relaxation of both orders of Legendre polynomials corresponding to BDS ($l = 1$) and DDLS ($l = 2$) experiments, but also rarely experimentally accessible *single*-molecule (self-)correlation functions ($l = 1, 2$), and complementary (unmeasurable) cross-contributions ($l = 1, 2$) can be determined. Moreover, the freedom of shaping the molecules provides a way to modify steric interactions, while changing the magnitude of their dipole moment allows to tune the interparticle interactions. However, to make our computational studies as general as possible, the chosen model molecule should be highly symmetrical (which is not considered to be a model of the experimentally studied molecules OTP and DVC), but simultaneously it must possess the dipole moment. Taking both issues into account, we employ the model of quasireal tetrahedron-like molecule, which consists of five identical atoms [47–50]. One of them is in the center of the tetrahedron, whereas others are placed in its corners, which makes the sphere reasonably describe the TM's shape; consequently, the role of the shape irregularity in molecular dynamics is substantially suppressed. Dipole moment is provided by assigning opposite charges to two different atoms (the central- and a side one).

We start the analysis of the time-dependent correlation functions from the $C^{BDS}(t)$, which can be expressed as a sum of the self- and cross-correlation functions [Eq. (1)]. The latter implies that the estimation of the cross-term, for which direct calculation requires enormous computational effort, can be done by subtracting the easily accessible self- component from the total correlation functions. In Fig. 5 we present the obtained $C^{BDS}(t)$ and its self- component. To improve statistics of $C^{BDS}(t)$, which is a macroscopic quantity, the presented data were averaged over 25 independent simulation runs (all of those runs were preceded by the equilibration of the systems).

From Fig. 6 it can be simply deduced that the contribution of the self-component to the C^{BDS} is at the level of about

20%, which means that the cross-term evidently dominates in the BDS response. As a consequence, we can state that our model system exhibits strong dipole-dipole cross-correlations. Taking the above into account, the crucial question is whether they are observed also in the DDLS response function. The correlation functions $C^{DDLS}(t)$ and $C_{self}^{DDLS}(t)$ calculated for our TM system [Eq. (2)] are presented in Fig. 6. Considering the relatively low amplitude of $C_{self}^{DDLS}(t)$, it is clear that $C^{DDLS}(t)$ contains a substantial contribution from cross-correlations. The amplitude of the $C_{self}^{DDLS}(t)$ is higher than $C_{self}^{BDS}(t)$; nevertheless, it is still at the level of 40%, which indicates that the role of cross-term is comparable to the that of the self- term and therefore, it cannot be neglected even for quite simple, highly symmetrical molecules. On the basis of the amplitude values of the self- components of the correlation functions, we estimated the values of $g_1 = 5$ and $g_2 = 2.5$. This general result must be highlighted, especially if one considers the recent papers that also study the role of the cross-term in $C^{DDLS}(t)$. In Ref. [46] we show that the magnitude of the cross-term is not only substantially smaller but also negligible for model molecules of the asymmetric shape, which possesses the dipole moment oriented alongside the longest molecular axis. Similar results are also reported for glycerol in Ref. [51], where the authors pointed out that in the DDLS experiment, the effect of cross-correlation is very weak, and the total loss function can reasonably be assimilated to the self- loss function. Consequently, the comparison between the collective dynamics probed by BDS and DDLS dynamic is not as trivial as suggested. The role of the molecular structure, the orientation of the polarizability tensor, and H bonds are only a few factors which might influence the $C_{cross}^{DDLS}(t)$ magnitude. Nevertheless, we can conclude that in general, the contribution of $C_{cross}^{DDLS}(t)$ cannot be simply neglected, which might be the immediate reason why BDS and DDLS experiments return similar values of the relaxation time for DVC.

As the last step of our studies, we examine the shear spectra of OTP and DVC, to check whether they also superpose with BDS and DVC data. As presented in Fig. 7, the real and imaginary parts of shear modulus data, i.e., G' and G'', recorded in the supercooled-liquid state of OTP and DVC satisfy the time-temperature superposition. Additionally, the loss modulus of both systems can be satisfactorily described by the KWW function with the stretch exponential equal to 0.6.

From the data presented in Fig. 7, one can conclude that the width of G'' does not depend on the μ value. Consequently, in this case the mechanical response seems to be insensitive to dipole-dipole cross correlations. Interestingly, β_{KWW} determined from shear experiment of both examined samples corresponds well with their β_{KWW}^{DDLS}. Consequently, G'' spectrum of OTP is also narrower than the dielectric one. So far, this situation has also been observed for weakly polar polymer polybutadiene [42]. However, in this context, one should remember that the shear experiment is sensitive to translation and rotation of molecules, whereas both BDS and DDLS probe only the molecular reorientations. The relaxation times obtained from the mechanical measurements are also presented in Fig. 5, where one can compare them with those determined from BDS and DDLS experiments. At first glance,
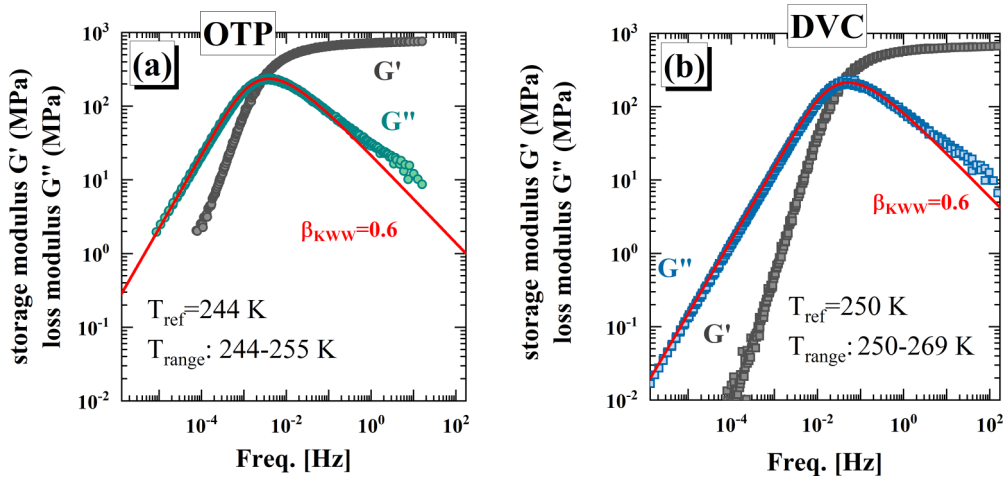
FIG. 7. Storage and loss modulus data recorded in the vicinity of liquid-glass transition of OTP (a) and DVC (b) presented in the form of master curve.

it can also be noted that for OTP, taking into account the κ parameter, there is a satisfying agreement between all measured timescales, τ_α^G, $\tau_\alpha^{BDS} = 1/\omega_{max}$, and $\tau_\alpha^{DDLS} = \langle\tau^{DDLS}\rangle$. At the same time, for DVC the mechanical relaxation times deviate slightly from DDLS and BDS results, especially at higher temperatures. Moreover, the high value of the ratio $\langle\tau^{DDLS}\rangle/\langle\tau^{BDS}\rangle$ strongly suggests that the orientational correlations in DVC are more pronounced in the DDLS dynamics.

V. CONCLUSIONS

In this paper we examined the molecular dynamics of two glass-forming liquids with similar chemical structures but remarkably different dipole-moment values. The first, abbreviated as OTP, is considered a canonical weakly polar glass former, while the second, called herein DVC, can be treated as its polar counterpart. A high dipole-moment ($5.3D$) value of the latter compound is provided by the dioxolane ring substituting the middle phenyl ring of OTP. At the same time, OTP and DVC can be regarded as highly optically anisotropic molecules due to the remaining two phenyl groups. Considering recent literature suggestion on the origin of BDS and DDLS spectra we could suspect that results of both experiments would be similar for OTP, whereas they would significantly differ for DVC. Indeed, our examinations have shown that an increase in the μ value makes the dielectric permittivity spectrum narrower, while it does not affect the DDLS susceptibility spectral shape. The latter trend has also been followed by shear experiments showing identical shapes of $G''(f)$ spectra for both systems. However, a good agreement (after correction with κ) between DDLS and dielectric relaxation times has been obtained for OTP, while for highly polar DVC no orientational correlations were detected from BDS measurements; simultaneously, $g_2 = 2$ was estimated from the

comparison of mean relaxation times [Eq. (6)]. This result is not surprising for OTP since only self-correlation contribution to dielectric spectra was postulated for weakly polar glass formers but the relation found between $\langle\tau^{DDLS}\rangle$ and $\langle\tau^{BDS}\rangle$ for the highly polar DVC is at odds with reverse separation between these two timescales reported for TBP. We should note, however, that the data reported for TBP suggest that the mean relaxation times measured by BDS and DDLS for TBP seem to be moderately, rather than strongly, separated. Note that DVC and TBP are characterized by the same dielectric strength ($\Delta\varepsilon = 20$). The different polarizability due to the lack of aromatic moieties in the chemical structure of the latter one affects only the level of the DDLS signal and not the degree of correlations. The explanation herein presented result is that cross-correlations may also give a substantial contribution to the DDLS response, as expected for a method measuring the collective dynamics. Judging from the mean relaxation time values and assuming the standard value of κ, we deduce twice-larger correlations visible in BDS compared to DDLS for TBP while twice-larger contribution of the cross-term in DDLS for DVC. Moreover, the value of g_1 obtained from ε' measurements for DVC indicates effective (apparent) lack of correlations detected by BDS. The results of the performed computational studies of model systems clearly show that the contribution of the cross-correlations to the total (collective) correlation function probed by the DDLS experiment can be substantial for polar molecules.

ACKNOWLEDGMENT

[1] P. Lunkenheimer, U. Schneider, R. Brand, and A. Loid, Contemp. Phys. **41**, 15 (2000).

[2] M. Paluch, B. Yao, J. Pionteck, and Z. Wojnarowska, Phys. Rev. Lett. **131**, 086101 (2023).

[3] F. Kremer and A. Schönhals, *Broadband Dielectric Spectroscopy* (Springer Berlin, Berlin, 2003).

[4] B. J. Berne and R. Pecora, *Dynamic Light Scattering: With Applications to Chemistry, Biology, and Physics* (Dover Publications, Mineola, NY, 2000).

[5] A. Patkowski, W. Steffen, H. Nilgens, E. W. Fischer, and R. Pecora, J. Chem. Phys. **106**, 8401 (1997).

[6] K. Zero and R. Pecora, in *Dynamic Light Scattering*, Applications of Photon Correlation Spectroscopy, edited by R. Pecora (Springer, NewYork, NY, 1985), pp. 59–83.

[7] G. P. Johari and M. Goldstein, J. Chem. Phys. **53**, 2372 (1970).

[8] K. L. Ngai and M. Paluch, J. Chem. Phys. **120**, 857 (2003).

[9] K. L. Ngai, R. Casalini, S. Capaccioli, M. Paluch, and C. M. Roland, J. Phys. Chem. B **109**, 17356 (2005).

[10] A. S. Volkov, G. D. Koposov, R. O. Perfil'ev, and A. V. Tyagunin, Opt. Spectrosc. **124**, 202 (2018).

[11] M. Paluch, J. Knapik, Z. Wojnarowska, A. Grzybowski, and K. L. Ngai, Phys. Rev. Lett. **116**, 025702 (2016).

[12] J. Gabriel, F. Pabst, A. Helbling, T. Böhmer, and T. Blochowicz, in *The Scaling of Relaxation Processes. Advances in Dielectrics*, edited by F. Kremer and A. Loidl (Springer International Publishing, Cham, 2018), pp. 203–245.

[13] A. Brodin, R. Bergman, J. Mattsson, and E. A. Rössler, Eur. Phys. J. B - Condens. Matter Complex Syst. **36**, 349 (2003).

[14] Y. Wang, P. J. Griffin, A. Holt, F. Fan, and A. P. Sokolov, J. Chem. Phys. **140**, 104510 (2014).

[15] J. S. Hansen, A. Kisliuk, A. P. Sokolov, and C. Gainaru, Phys. Rev. Lett. **116**, 237601 (2016).

[16] F. Pabst, A. Helbling, J. Gabriel, P. Weigl, and T. Blochowicz, Phys. Rev. E **102**, 010606(R) (2020).

[17] F. Pabst, J. P. Gabriel, T. Böhmer, P. Weigl, A. Helbling, T. Richter, P. Zourchang, T. Walther, and T. Blochowicz, J. Phys. Chem. Lett. **12**, 3685 (2021).

[18] T. Keyes, Mol. Phys. **23**, 737 (1972).

[19] P.-M. Déjardin, S. V. Titov, and Y. Cornaton, Phys. Rev. B **99**, 024304 (2019).

[20] P. M. Déjardin, Y. Cornaton, P. Ghesquière, C. Caliot, and R. Brouzet, J. Chem. Phys. **148**, 044504 (2018).

[21] S. A. Yamada, H. E. Bailey, and M. D. Fayer, J. Phys. Chem. B **122**, 12147 (2018).

[22] D. V. Matyushov and R. Richert, J. Phys. Chem. Lett. **14**, 4886 (2023).

[23] E. N. Ivanov, Sov. Phys. JETP **18**, 1041 (1964).

[24] W. C. Ehrhardt and W. E. Vaughan, J. Chem. Phys. **74**, 5479 (1981).

[25] A. Jedrzejowska, Z. Wojnarowska, K. Adrjanowicz, K. L. Ngai, and M. Paluch, J. Chem. Phys. **146**, 094512 (2017).

[26] A. Tölle, Rep. Prog. Phys. **64**, 1473 (2001).

[27] W. L. Jorgensen, D. S. Maxwell, and J. Tirado-Rives, J. Am. Chem. Soc. **118**, 11225 (1996).

[28] H. Bekker, H. J. C. Berendsen, E. J. Dijkstra, S. Achterop, R. Vondrumen, D. Vanderspoel, A. Sijbers, H. Keegstra, and M. K. R. Renardus, *Phys. Comput. '92*, edited by R. DeGroot and J. Nadrchal (World Scientific Publishing, Singapore, 1993), pp. 252–256.

[29] H. J. C. Berendsen, D. van der Spoel, and R. van Drunen, Comput. Phys. Commun. **91**, 43 (1995).

[30] D. Van Der Spoel, E. Lindahl, B. Hess, G. Groenhof, A. E. Mark, and H. J. C. Berendsen, J. Comput. Chem. **26**, 1701 (2005).

[31] S. Páll, M. J. Abraham, C. Kutzner, B. Hess, and E. Lindahl, in *Solving Software Challenges Exascale Int. Conf. Exascale Appl. Software, EASC 2014*, edited by S. Markidis and E. Laure (Springer International Publishing, Cham, 2015), pp. 3–27.

[32] M. J. Abraham, T. Murtola, R. Schulz, S. Páll, J. C. Smith, B. Hess, and E. Lindahl, SoftwareX **1**, 19 (2015).

[33] S. Nosé, Mol. Phys. **52**, 255 (1984).

[34] S. Nosé, J. Chem. Phys. **81**, 511 (1984).

[35] W. G. Hoover, Phys. Rev. A **31**, 1695 (1985).

[36] L. Verlet, Phys. Rev. **159**, 98 (1967).

[37] T. Darden, D. York, and L. Pedersen, J. Chem. Phys. **98**, 10089 (1993).

[38] R. Richert, J. Chem. Phys. **123**, 154502 (2005).

[39] C. León and K. L. Ngai, J. Phys. Chem. B **103**, 4045 (1999).

[40] W. Steffen, A. Patkowski, G. Meier, and E. W. Fischer, J. Chem. Phys. **96**, 4171 (1992).

[41] N. Petzold and E. A. Rössler, J. Chem. Phys. **133**, 124512 (2010).

[42] K. L. Ngai, Z. Wojnarowska, and M. Paluch, Sci. Rep. **11**, 22142 (2021).

[43] L. Simeral and R. L. Amey, J. Phys. Chem. **74**, 1443 (1970).

[44] J. Świergiel, I. Płowaś, and J. Jadżyn, J. Mol. Liq. **220**, 879 (2016).

[45] J. Świergiel, I. Płowaś, and J. Jadżyn, J. Mol. Liq. **223**, 628 (2016).

[46] K. Koperwas and M. Paluch, Phys. Rev. Lett. **129**, 025501 (2022).

[47] M. Paluch, K. Koperwas, and Z. Wojnarowska, J. Mol. Liq. **382**, 121907 (2023).

[48] K. Koperwas, A. Grzybowski, and M. Paluch, Phys. Rev. E **101**, 012613 (2020).

[49] K. Koperwas, A. Grzybowski, and M. Paluch, Phys. Rev. E **102**, 062140 (2020).

[50] F. Kaśkosz, K. Koperwas, and M. Paluch, J. Mol. Liq. **366**, 120321 (2022).

[51] M. Hénot, P.-M. Déjardin, and F. Ladieu, Phys. Chem. Chem. Phys. **25**, 29233 (2023).